

The value of polarization in camera-based photoplethysmography

ALEXANDER TRUMPP,^{1,*} PHILIPP L. BAUER,¹ STEFAN RASCHE,²
HAGEN MALBERG,¹ AND SEBASTIAN ZAUNSEDER¹

¹Institute of Biomedical Engineering, Faculty of Electrical and Computer Engineering, Technische Universität Dresden, 01062 Dresden, Germany

²Herzzentrum Dresden, Department of Cardiac Surgery, Faculty of Medicine Carl Gustav Carus, Technische Universität Dresden, 01062 Dresden, Germany

*alexander.trumpp@tu-dresden.de

Abstract: Camera-based photoplethysmography (cbPPG) is a novel measuring technique that permits the remote acquisition of cardiovascular signals using video cameras. Research still lacks in fundamental studies to reach a deeper technical and physiological understanding. This work analyzes the employment of polarization filtration to (i) assess the gain for the signal quality and (ii) draw conclusions about the cbPPG signal's origin. We evaluated various forehead regions of 18 recordings with different color and filter settings. Our results prove that for an optimal illumination, the perpendicular filter setting provides a significant benefit. The outcome supports the theory that signals arise from blood volume changes. For lateral illumination, ballistocardiographic effects dominate the signal as polarization's impact vanishes.

© 2017 Optical Society of America

OCIS codes: (170.3660) Light propagation in tissues; (170.3880) Medical and biological imaging; (280.0280) Remote sensing and sensors

References and links

1. M. Huelsbusch and V. Blazek, "Contactless mapping of rhythmical phenomena in tissue perfusion using PPGI," *Proc. SPIE* **4683**, 110–117 (2002).
2. F. P. Wieringa, F. Mastik, and A. F. W. van der Steen, "Contactless Multiple Wavelength Photoplethysmographic Imaging: A First Step Toward "SpO2 Camera" Technology," *Annals of Biomedical Engineering* **33**(8), 1034–1041 (2005).
3. J. Allen, "Photoplethysmography and its application in clinical physiological measurement," *Physiol. Meas.* **28**(3), R1 (2007).
4. C. Takano and Y. Ohta, "Heart rate measurement based on a time-lapse image," *Medical Engineering & Physics* **29**(8), 853–857 (2007).
5. W. Verkruysse, L. O. Svaasand, and J. S. Nelson, "Remote plethysmographic imaging using ambient light.," *Opt. Express* **16**(26), 21434–21445 (2008).
6. S. G. Demos and R. R. Alfano, "Optical polarization imaging," *Appl. Opt.* **36**(1), 150–155 (1997).
7. W. Groner, J. W. Winkelman, A. G. Harris, C. Ince, G. J. Bouma, K. Messmer, and R. G. Nadeau, "Orthogonal polarization spectral imaging: A new method for study of the microcirculation," *Nature Medicine* **5**(10), 1209–1212 (1999).
8. S. Jacques, J. C. Ramella-Roman, and K. Lee, "Imaging skin pathology with polarized light," *J. Biomed. Opt.* **7**(3), 329–340 (2002).
9. R. R. Anderson, "Polarized Light Examination and Photography of the Skin," *Archives of Dermatology* **127**(7), 1000–1005 (1991).
10. A. A. Kamshilin, V. Teplov, E. Nippolainen, S. Miridonov, and R. Giniatullin, "Variability of microcirculation detected by blood pulsation imaging," *PLoS One* **8**(2), e57117 (2013).
11. N. Zaproudina, V. Teplov, E. Nippolainen, J. A. Lipponen, A. A. Kamshilin, M. Närhi, P. A. Karjalainen, and R. Giniatullin, "Asynchronicity of Facial Blood Perfusion in Migraine," *PLoS One* **8**(12), e80189 (2013).
12. A. A. Kamshilin, E. Nippolainen, I. S. Sidorov, P. V. Vasilev, N. P. Erofeev, N. P. Podolian, and R. V. Romashko, "A new look at the essence of the imaging photoplethysmography," *Sci. Rep.* **5**, 10494 (2015).
13. A. A. Kamshilin, I. S. Sidorov, L. Babayan, M. A. Volynsky, R. Giniatullin, and O. V. Mamontov, "Accurate measurement of the pulse wave delay with imaging photoplethysmography," *Biomed. Opt. Express* **7**(12), 5138–5147 (2016).
14. S. Xu, L. Sun, and G. Rohde, "Robust efficient estimation of heart rate pulse from video," *Biomed. Opt. Express* **5**(4), 1124–1135 (2014).

15. A. V. Moço, S. Stuijk, and G. de Haan, "Skin inhomogeneity as a source of error in remote PPG-imaging," *Biomed. Opt. Express* **7**(11), 4718–4733 (2016).
16. A. V. Moço, S. Stuijk, and G. de Haan, "Ballistocardiographic Artifacts in PPG Imaging," *IEEE Transactions on Biomedical Engineering* **63**(9), 1804–1811 (2016).
17. A. V. Moço, S. Stuijk, and G. de Haan, "Motion robust PPG-imaging through color channel mapping," *Biomed. Opt. Express* **7**(5), 1737–1754 (2016).
18. Z. Marcinkevics, U. Rubins, J. Zaharans, A. Miscuks, E. Urtane, and L. Ozolina-Moll, "Imaging photoplethysmography for clinical assessment of cutaneous microcirculation at two different depths," *J. Biomed. Opt.* **21**(3), 035005 (2016).
19. M. Huelsbusch, "An image-based functional method for opto-electronic detection of skin-perfusion," Phd thesis, RWTH Aachen dept. of EE. (in German) (2008).
20. I. S. Sidorov, M. A. Volynsky, and A. A. Kamshilin, "Influence of polarization filtration on the information readout from pulsating blood vessels," *Biomed. Opt. Express* **7**(7), 2469–2474 (2016).
21. A. Reisner, P. A. Shaltis, D. McCombie, and H. H. Asada, "Utility of the Photoplethysmogram in Circulatory Monitoring," *Anesthesiology* **108**(5), 950–958 (2008).
22. A. N. Bashkatov, E. A. Genina, V. I. Kochubey, and V. V. Tuchin, "Optical properties of human skin, subcutaneous and mucous tissues in the wavelength range from 400 to 2000 nm," *Journal of Physics D: Applied Physics* **38**(15), 2543–2555 (2005).
23. Y. Dancik, P. L. Bigliardi, and M. Bigliardi-Qi, "What happens in the skin? Integrating skin permeation kinetics into studies of developmental and reproductive toxicity following topical exposure," *Reproductive Toxicology* **58**, 252–281 (2015).
24. Arthur C. Guyton and John E. Hall, *Textbook of Medical Physiology* (Elsevier Health Sciences, 2006), Chap. 4.
25. T. Lister, P. A. Wright, and P. H. Chappell, "Optical properties of human skin," *J. Biomed. Opt.* **17**(9), 90901-1 (2012).
26. L. Giovangrandi, O. T. Inan, R. M. Wiard, M. Etemadi, and G. T. A. Kovacs, "Ballistocardiography – A Method Worth Revisiting," *Proceedings of Annual International Conference of the IEEE Engineering in Medicine and Biology Society* (IEEE, 2011), pp. 4279–4282.
27. H. Liu, Y. Wang, and L. Wang, "The Effect of Light Conditions on Photoplethysmographic Image Acquisition Using a Commercial Camera," in *IEEE Journal of Translational Engineering in Health and Medicine* **2**, 1–11 (2014).
28. R. Sameni, "OSET - The Open-Source Electrophysiological Toolbox," (version 2.1, 2010), <http://www.oset.ir>.
29. G. Lempe, S. Zaunseder, T. Wirthgen, S. Zipser, and H. Malberg, "ROI Selection for Remote Photoplethysmography," in *Proceedings of Bildverarbeitung für die Medizin 2013* (Springer, 2013), pp. 99–103.
30. W. Cui, L. E. Ostrander, and B. Y. Lee, "In vivo reflectance of blood and tissue as a function of light wavelength," *IEEE Transactions on Biomedical Engineering* **37**(6), 632–639 (1990).
31. L. F. Corral, G. Paez, and M. Strojnik, "Optimal wavelength selection for noncontact reflection photoplethysmography," *Proc. SPIE* **8011**, 801191 (2011).

1. Introduction

Camera-based photoplethysmography (cbPPG) is an optical measuring technique that allows the remote acquisition of cardio-respiratory signals using common video cameras [1, 2]. The underlying principle is similar to the one in regular photoplethysmography (PPG) where back-scattered light from superficial skin layers, which is modulated by physiological processes, is captured and converted into signals [3]. Both, cbPPG and PPG function with light in the visible and near-infrared spectrum. In contrast to PPG, cbPPG can also be operated without a dedicated light source simply using ambient light [4, 5]. Furthermore, the two-dimensional camera sensor enables the extraction of spatially separated information overcoming the limitation of a punctual measurement [2, 5]. Although cbPPG could be applied in contact with the skin, we give priority to the remote setting in which the subject is not disturbed by any instrumentation.

In the last decade, cbPPG gained a lot of attention due to its convenient and simple setup. Most works focus on software development to ensure a reliable employment in different environments. The potential of hardware adjustments, however, is rarely addressed. In that respect, polarization filtration opens up new perspectives as already used in various imaging techniques [6–8]. These techniques exploit the fact that marginally scattered light keeps its state of polarization while strongly scattered light loses the state. Consequently, (i) the application of two filters with the same polarization direction at the camera and light source (parallel setting) allows the analysis of the skin surface, and (ii) the perpendicular alignment (perpendicular setting) allows the analysis

of skin tissue beneath the surface [9]. Previous works in cbPPG applied the perpendicular setting to suppress specular reflectance from the skin surface [10–18]. However, investigations that systematically assess the benefit of polarization filtration for cbPPG are rare. Huelsbusch [19] tested linear polarization in a perpendicular setting but could not show any improvements in the signal quality. Sidorov et al. [20] compared the perpendicular setting versus a setting without filters for the palm which was compressed against a glass plate. They reported a reduction of noise and artifacts but no significant increase in the blood pulsation amplitude when using polarization filtration.

Besides a potential benefit for practical applications, polarization filtration might also yield valuable information regarding the origin of cbPPG signals. Various theories have been discussed in the past attempting to shed more light on factors that modulate the detected signal. One theory relies on the classic PPG theory in which the main contribution of the signal's pulsation component arises from the arterial vasculature [21]. For cbPPG, wavelengths in the red, green and blue range are of particular interest since RGB cameras are a convenient choice for the technique. Blue (450 nm) and green light (520 nm) penetrate the skin up to a depth of 0.7 mm and 0.9 mm, respectively, allowing these wavelengths to interact with arterioles in the reticular dermis [22, 23]. Only red light (630 nm) with a penetration depth of 1.8 mm likely reaches down to the deep net plexus where already small arteries can be found [22, 23]. However, both types of vessels, arterioles and arteries, are compliant and pulsate in accordance with the cardiac cycle [24]. The periodic change of vessels' cross-section changes the blood volume insight the recording area. This blood volume change modulates the incoming light where hemoglobin plays the key role due to its high absorption value [25]. Another theory was proposed by Kamshilin et al. [12] who diverged from the classic model. The group addressed the green light range and claimed that there is a low probability for respective wavelengths to interact with pulsating vessels. They proposed a model in which the oscillation of the transmural pressure in larger and deeper arteries leads to a periodical deformation of the adjacent tissue in the dermis. The deformation changes the density of this tissue, including the density of capillaries in the papillary dermis. The density change also affects the blood volume inside the recording area regardless of the fact that capillaries are non-compliant [24]. Although both theories take different types of vessels into account, blood volume changes are acknowledged to be the primary factor for the modulation of cbPPG signals (further on referred to as 'blood volume effect'). Another factor which additionally might have a strong impact is represented by ballistocardiographic (BCG) effects [26]. These effects can superimpose with blood volume effects which complicate the interpretation regarding the cbPPG signal's origin. Moço et al. [16, 17] showed BCG effects to occur more and stronger in case of non-orthogonal (incident light not at a right angle with skin surface) and inhomogeneous illumination. In contrast to blood volume effects, they are detectable on the skin surface and do not require the light's interaction with the vasculature. As already suggested before, polarization filtration offers a way to distinguish between specific skin layers. In combination with a systematic color setting, it provides an opportunity to identify certain effects and shed more light on the origin of cbPPG signals.

In this work, we evaluate the benefit of polarization filtration for cbPPG using wavelengths in the red, green and blue color range. To the best of our knowledge, there are no equivalent investigations in the field where considered skin tissue was not compressed. The goal of our study is (i) to analyze which filter setting leads to the highest increase in signals' pulse strength, and (ii) to draw conclusions about signal's origin by exploiting different filter and color settings. We believe the results to contribute extensively to a systematic employment of polarization filtration in future works. Moreover, the better fundamental understanding of cbPPG will allow a better adaption of methods to specific applications.

2. Material and methods

2.1. Technical setup and data

For illumination, we designed and built an LED matrix (140 mm × 230 mm) which holds 6 × 9 single RGB LEDs of the type SFT722N-S. The LEDs are driven by a constant current to avoid unwanted flickering in the videos. Each color can be adjusted separately to a certain intensity between zero and maximal power. Further technical specifications are listed in Table 1. The matrix was the only light source during the measurements. For video recording, we used a monochrome industrial camera (IDS UI-3370CP-NIR-GL) that was equipped with a lens by Schneider-Kreuznach (Cinegon 16/1.8). The camera was set to a resolution of 420 × 320 pixels, a color depth of 12 bits, a frame rate of 50 fps and an exposure time of 20 ms. All videos were stored in an uncompressed binary format and further processed using MATLAB 2016a. Depending on the test in the experiment, linear polarization filters were fixed to the illumination matrix and the camera, respectively. We used a customized polarization film (Schneider-Kreuznach P-W76) for the matrix which was slid into a slot of the case. The polarization direction was oriented vertically. For the camera, a glass filter (Schneider-Kreuznach M30.5x0.5 IF AUF) was applied and mounted on the front of the lens. The polarization direction was varied between a parallel and perpendicular orientation regarding the direction of the film filter. Additional filter information can be found in Table 1. As a reference, we recorded PPG signals that were obtained by an ear clip (ADInstruments, MLT1020EC) using the PowerLab 16/35 (ADInstruments, Dunedin, NZ). Both, video and PPG data were captured synchronously on a PC.

Table 1. Technical specifications for the used LED matrix and the applied polarization filters.

		Blue	Green	Red
LED	Electrical power	5.2 W	5.2 W	3.4 W
	Peak wavelength	453 nm	518 nm	632 nm
	Spectral bandwidth	23 nm	33 nm	14 nm
Polarization filter	Extinction ratio glass	300	7000	100000
	Extinction ratio film	1000	8000	70000

We recruited 18 Caucasian volunteers (17 male, 1 female) between 21 and 29 years (25.2 ± 2.2 years). Each individual was informed about the measurements' procedure and gave written consent. The study was approved by the Institutional Review Board of the TU Dresden (IRB00001473, EK168052013). For the experiment, the subjects were positioned in front of the illumination matrix and the camera at a distance of approximately 450 mm. They were asked to comfortably rest their head on a soft pillow, which was placed on a desk, and remain relaxed and steady during the measurements. The matrix and the camera were aligned towards the forehead which was chosen as the region of interest (ROI). An additional hair circlet prevented any ROI occlusion by the hair. Furthermore, our protocol required to wear safety goggles in order to avoid eye irritation. The recording area contained mostly the upper part of the face and, to some extent, also the background. The whole experimental setup is depicted in Fig. 1.

2.2. Experimental procedure

For each subject, nine subsequent tests of 20 s were conducted. At first, three tests were performed using the perpendicular filter setting (denoted by '+'), followed by three tests where the parallel setting was applied (denoted by '||'). The last three tests were executed using no polarization filters (denoted by 'o'). In each of the three subtests, a different color was set at the illumination matrix: i) blue, ii) green and iii) red. Note that the LEDs were operated at their maximal output. Liu et al. [27] showed that the image intensity affects the quality of extracted cbPPG signals. Due to changing filter and color settings in our analysis, the mean image intensity would vary.

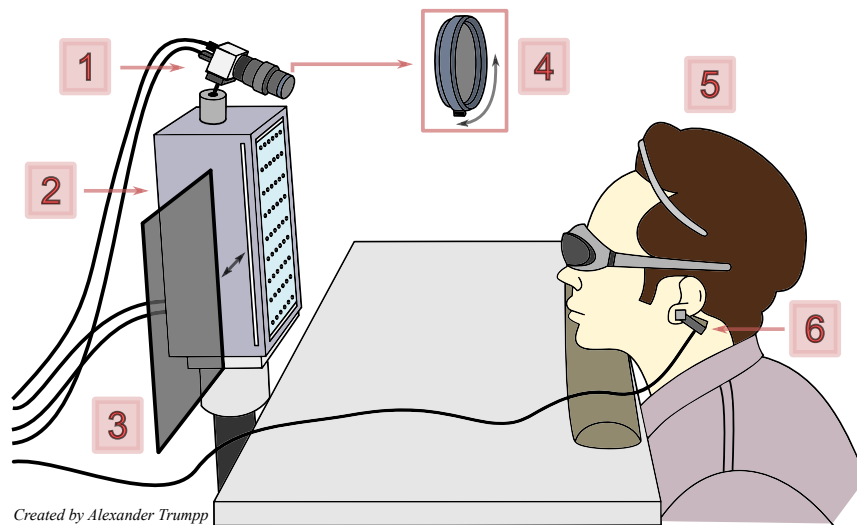


Fig. 1. Measuring setup of the polarization experiment: 1) Camera system, 2) Multi-wavelength illumination matrix, 3) Polarization filter (film), 4) Polarization filter (glass) with an adaptable angle, 5) Test subject with protection goggles and hairband, 6) Reference PPG sensor.

Therefore, before each test, we manually adjusted the aperture of the lens to obtain a similar ROI intensity ensuring a higher comparability between the tests. During the adjustment, we also guaranteed that the forehead was not locally under or oversaturated.

2.3. Image and signal processing

For each subject, we manually defined one ROI for the forehead which was determined in the first frame of the first test. The ROI was then held statically over the test. We used the same ROI for the following tests but corrected the position in the corresponding first frame if necessary. During the annotation, we tried not to include high-contrast areas like skin edges. Figure 2(a) shows an example. In further descriptions, the forehead ROI will be denoted by ROI_{full} . In order to take regional differences into account, we also applied spatially distributed ROIs (size of 15×15 pixels) which were automatically fitted in ROI_{full} of each subject. An example can be found in Fig. 2(b). Across all subjects, between 49 and 133 (90 ± 24.6) blocks were defined that will be referred to as $ROI_{i,small}$ (i is the ROI number). By comparing the performance of the ROI blocks, we aimed at finding systematic characteristics which are worth looking into and which should be considered for a substantial analysis. Based on the results (see Fig. 3, red wavelength) and prior knowledge about BCG influences at lateral areas [16], we determined three larger ROIs that were set to be evaluated in depth along with ROI_{full} . Two regions ROI_{left} and ROI_{right} were positioned at the left and right side of the forehead holding a width of 30 pixels (empirically chosen). The third region ROI_{center} was defined as a reference with the same width and aligned in the middle of ROI_{left} and ROI_{right} . The three ROIs are confined by ROI_{full} , and they all have similar sizes ensuring a better comparability between the results (see Fig. 2(c) for an example).

After annotation, the cbPPG signals were extracted by averaging the pixels inside the respective ROI for every frame. Consequently, for each test and ROI, we obtained one signal. The signals were then bandpass filtered using a Butterworth filter (order 5, cutoff 0.5 and 15 Hz) to suppress low-frequency variations and high-frequency noise. We decided to declare the pulse strength p_{AC} as the quality index for our cbPPG signals (similar to pulsation amplitude measures in other works [19,20]). For determination of p_{AC} , we firstly detected the beats within the signals.

To prevent any false detections, we utilized the reference PPG signals that were captured separately for each test. The minima positions of the reference signals, which were extracted by applying the OSET MaxSearch algorithm [28], were used to cut out the single cbPPG beats. We omitted beats if their height was bigger than 30 intensity units because the physiological origin of such a variation can be ruled out. The remaining beats were averaged to one mean beat. Eventually, the pulse strength p_{AC} was set as the distance between the absolute minimum and maximum of the mean beat resulting in one p_{AC} value for each test and ROI. Figure 2 exemplarily depicts the procedure for one signal. Since the reference-guided detection does not consider if the pulsation component is related to the cardiac cycle, we also calculated the noise level n_{AC} for comparison. Two different ROIs with similar size and illumination as ROI_{full} and $ROI_{left/right/center}$, respectively, were applied to the background in a reference measurement. We based this step on an analogous approach from Kamshilin et al. [10]. In the same way as p_{AC} , n_{AC} was determined for the extracted signals leaving two noise values, one for the full forehead ROI and one for the ROI strips. The values are visualized as magenta lines in Fig. 4.

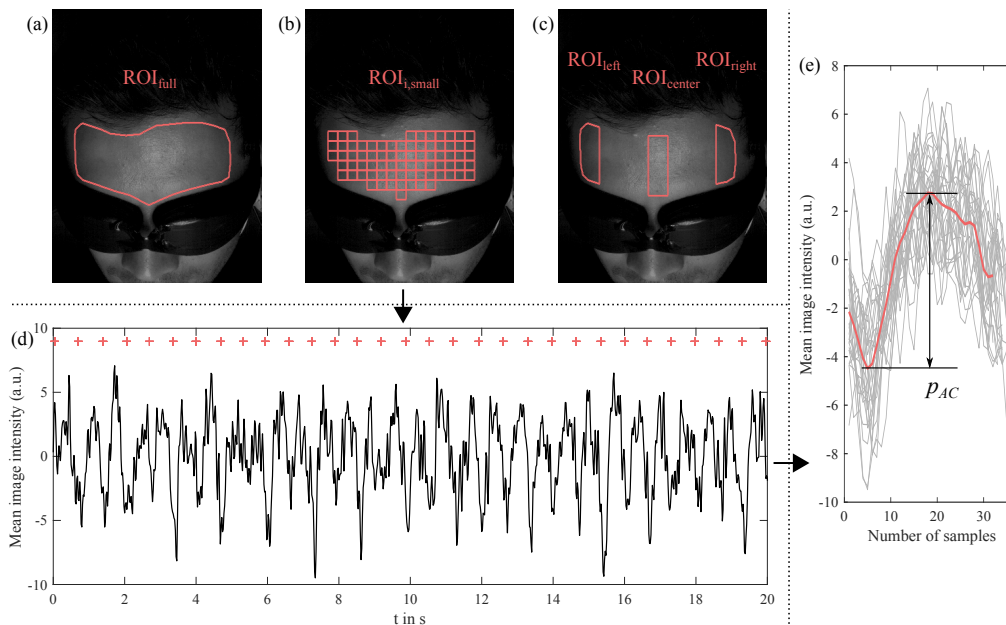


Fig. 2. Main processing steps depicted for an example: (a) Forehead ROI, (b) Equally sized sub-ROIs (15 x 15 pixels), (c) ROI strips that were defined based on the results when using the sub-ROIs, (d) Extracted cbPPG signal for one test with diastolic positions (red) of reference PPG, (e) Extracted beats and calculated mean beat (red) with the height p_{AC} .

2.4. Evaluation and statistics

Across all 18 subjects and nine experiments, we statistically analyzed the behavior of the p_{AC} values in each of the four ROIs (full, left, center, right). In order to assess whether the polarization filtration causes a significant change in p_{AC} , we applied a Friedman test separately for each color setting and ROI. If the Friedman test showed significance, post-hoc tests were performed using the Wilcoxon signed rank test where p-values were adjusted by the Bonferroni correction. Note that always three groups ('o', '|', '+') with 18 values were considered. In a second analysis, we evaluated the differences between the three wavelengths for each ROI and filter setting. Statistical testing was done over the respective three groups (blue, green, red) in the same way as in the first analysis. Eventually, a third analysis was performed to compare the results of the three ROI

strips since they were built due to local differences. For this purpose, three groups (left, middle, right) were taken into account for each color and filter setting and statistically tested as described above.

3. Results

The results of p_{AC} for the full forehead ROI are depicted in Fig. 4(a). The Friedman test shows that the polarization filtration leads to a significant change in signals' pulse strength within all three color settings (see Table 2, first column). The strongest differences can be found for blue and green, the lowest for red. As the post-hoc tests prove, the '+' setting yields signals with significant higher pulses p_{AC} than the '||' setting does. The same holds true for the '+' and 'o' setting with the exception of the red wavelengths. It should be noted that for red, the p_{AC} values accumulate around the noise level which makes their validity questionable. Blue is the only color to provide statistical differences between the 'o' and '||' setting although the trend for all colors implies the 'o' setting to perform better. When comparing the performance of the three wavelengths, substantial differences can be found (see Table 3, first column). The strongest ones occur with respect to red. The application of the green wavelengths provides the best outcome for p_{AC} . The values for blue are similarly high while the ones for red yield poor results.

Figure 3 shows the distribution of the pulse strength over the forehead within $ROI_{i,small}$ depicted exemplarily for three subjects and all tests. Mainly for the red wavelength, we noticed that high pulse strengths occur for the left and right area when comparing them to the center area. This effect led us to investigate these regions separately by applying and assessing ROI_{left} and ROI_{right} , as well as ROI_{center} for reference purposes (see also Section 2.3).

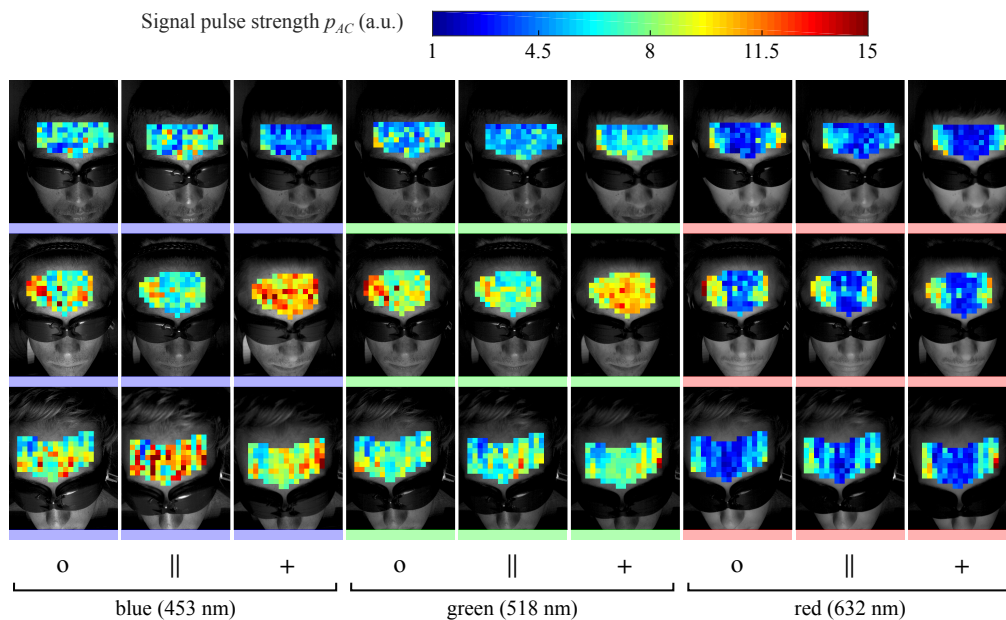


Fig. 3. Results for the spatio-temporal distribution of the pulse strength values (three subjects are depicted exemplarily). The values are false color coded where dark blue represents a low strength and dark red a high strength (see color map). The symbol 'o' represents the setting without polarization filters, '||' the parallel setting and '+' the perpendicular setting. The chosen color setting is represented by lines below the images and specified with their peak wavelengths (blue: 453 nm, green: 518 nm, red: 632 nm).

The results for the three ROI strips generally show larger p_{AC} values than we achieved for the full ROI (see Fig. 4(b) - (d)). The characteristics of the center ROI, with respect to the color and filter setting, are very similar to the ones of the full ROI. Apart from red, the polarization filtration proves again to have a significant impact on the outcome (see Table 2, column 3). The results of the post-hoc tests show minor irregularities. However, the lateral ROIs provide a more contradictory outcome. Whereas for the right ROI, the polarization seems to affect signal's pulse strength, for the left ROI, there are barely any differences between the filter settings (see Table 2, column 2 and 4). The applied post-hoc tests confirm this assessment. For the right ROI, the '+' setting is consistently better than '||' setting and, except for red, also better than the 'o' setting. When comparing the performance of the wavelengths (Table 3), no differences can be found on the left and the right side. The pulse strength values for red are substantially higher in these ROIs and reach the same level as blue and green do. Only for the center ROI, the results are significantly different between the colors, which is mainly caused by the poor performance of red. When comparing the three ROI locations (Table 4), a similar conclusion can be drawn. Exclusively for red, the left as well as the right region prove to provide significantly different results for all filter settings with respect to the center region. However, according to the tests, the lateral regions do not differ from each other. For green and blue, the results imply that there are no differences between the location regardless of which filter was used. Please note that we considered the factors 'filter setting', 'color setting' and 'ROI location' separately and that conclusions were drawn with regards to these factors.

4. Discussion

4.1. Impact of polarization filtration

Apart from the red wavelength and the left ROI, the '+' filter setting proved to provide signals with the highest pulse strengths, while the '||' setting consistently led to the lowest values. The outcome suggests that cbPPG signals hold higher qualities when the received light from the skin surface is eliminated. With respect to the performance of the 'o' setting, it can be similarly concluded that effects from the surface suppress the strength of signals from deeper skin layers. Our results deviate from the outcome of Huelsbusch [19] who found no improvements in the signal quality when using the '+' filter setting. Our findings also fundamentally disagree with the ones of Sidorov et al. [20]. They reported that the application of the '+' setting leads to no significant increase in the signal amplitude for the green wavelength. However, in their setup, the palm region was measured under external pressure, and only suitable ROIs (so-called hot spots) were taken into account. The pressure might play an important role in their outcome as we will discuss later (see Section 4.2). The influence of polarization differs across the forehead regions and almost vanishes at the left lateral ROI (see Fig. 4(b)-(d)). Nevertheless, the similarities between the full and the center ROI imply that the influence is still dominant in larger regions regardless of local differences. Smaller ROIs provide signals with stronger pulse strengths. Lempe et al. [29] already revealed this characteristic, which most likely originates from the fact that averaging over larger regions causes a suppression of local variations in the signal's morphology.

4.2. Origin of cbPPG signals

Color setting For the full and the center ROI, the blue and the green wavelengths provide the highest signal pulse strengths whereas the red wavelength yields the lowest strengths (see Fig. 4(a) and (c)). This behavior coincides with the absorption characteristic of hemoglobin [25] and, therefore, supports the theory that the cbPPG signal arises from blood volume changes (blood volume effect). However, compared to other investigations [30, 31], which multispectrally analyzed the cardiac strength of photoplethysmographic signals, the blue wavelength gives a

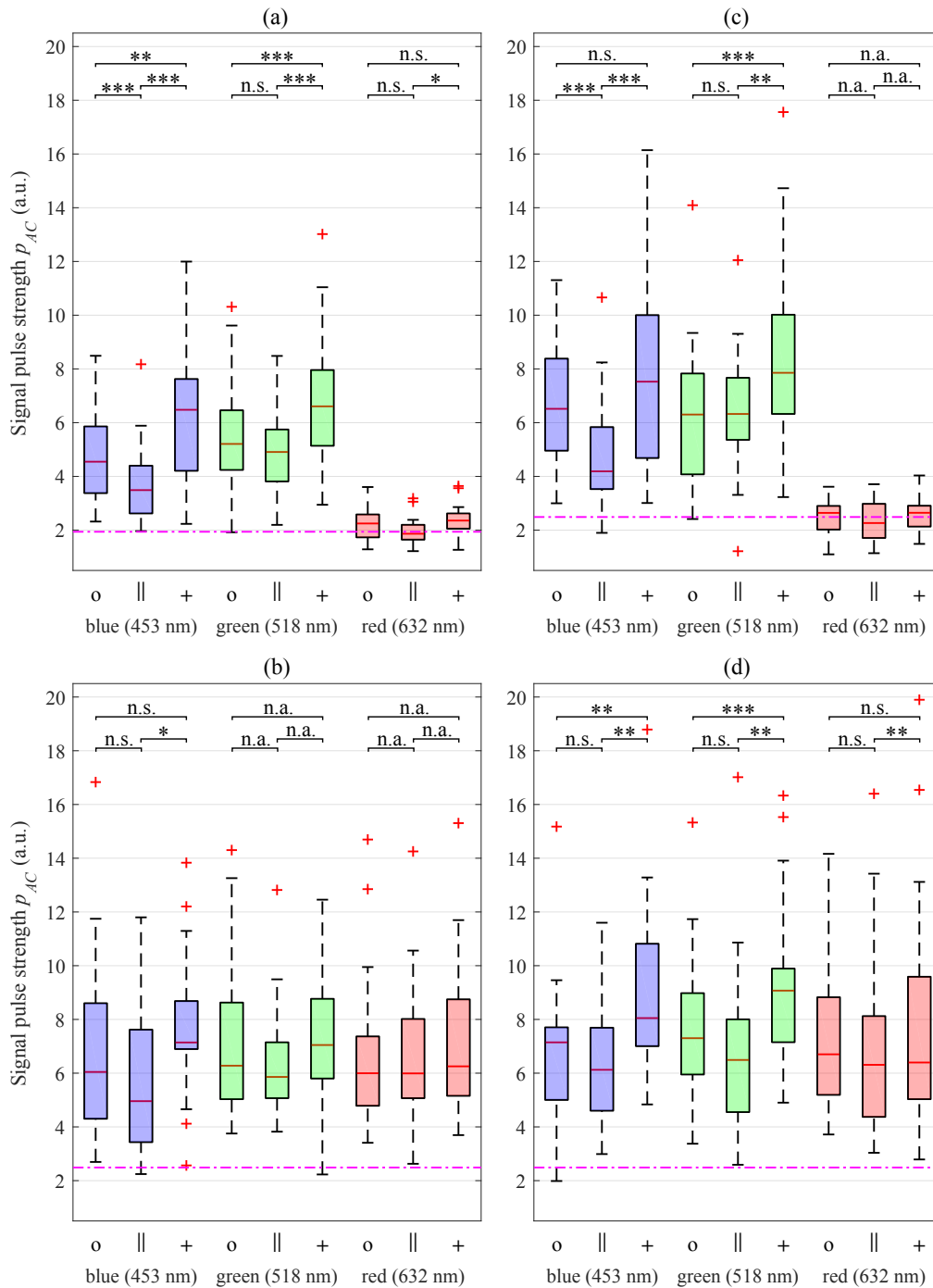


Fig. 4. Boxplot for the distribution of the pulse strength values: (a) Full forehead ROI, (b) Left ROI, (c) Center ROI, (d) Right ROI. The results of post-hoc tests (filtration) are also given (n.s. $p > 0.05$, * $p \leq 0.05$, ** $p \leq 0.01$, *** $p \leq 0.001$). If the post-hoc test was not applied, 'n.a.' is used. The symbol 'o' represents the setting without polarization filters, '||' the parallel setting and '+' the perpendicular setting. The chosen color setting is represented by boxes' coloration and specified with their peak wavelengths (blue: 453 nm, green: 518 nm, red: 632 nm). The magenta lines depict the noise level n_{AC} (see Section 2.3 for calculation).

Table 2. Results of the Friedman test to analyze the differences between groups of the same color but various filter settings (tests are performed across the filter settings). The values are given for all tested ROIs separately (full forehead, left, center and right region).

	ROI			
	Full	Left	Center	Right
Blue	***	**	***	***
Green	***	n.s.	***	***
Red	*	n.s.	n.s.	*

n.s. $p > 0.05$, * $p \leq 0.05$, ** $p \leq 0.01$, *** $p \leq 0.001$

Table 3. Results of the i) Friedman tests to analyze the differences between groups of the same filter setting but various colors (column 1), and ii) Post-hoc tests for the comparison of the three different colors for each ROI location (column 2-4). The symbol 'o' represents the setting without polarization filters, '||' the parallel setting and '+' the perpendicular setting.

		Color			
		All	Blue - Green	Blue - Red	Green - Red
Full	o	***	*	***	***
		***	**	***	***
	+	***	*	***	***
Left	o	n.s.	n.a.	n.a.	n.a.
		*	n.s.	n.s.	n.s.
	+	n.s.	n.a.	n.a.	n.a.
Center	o	***	n.s.	***	***
		***	**	***	***
	+	***	*	***	***
Right	o	n.s.	n.a.	n.a.	n.a.
		n.s.	n.a.	n.a.	n.a.
	+	n.s.	n.a.	n.a.	n.a.

n.a. post-hoc test not applied, n.s. $p > 0.05$, * $p \leq 0.05$, ** $p \leq 0.01$, *** $p \leq 0.001$

Table 4. Results of the i) Friedman test to analyze the differences between groups of the same color setting but various ROI locations (column 1), and ii) Post-hoc tests for the comparison of the three ROI locations (column 2-4). The symbol 'o' represents the setting without polarization filters, '||' the parallel setting and '+' the perpendicular setting.

		ROI			
		All	Left - Right	Left - Center	Right - Center
Blue	o	n.s.	n.a.	n.a.	n.a.
		n.s.	n.a.	n.a.	n.a.
	+	n.s.	n.a.	n.a.	n.a.
Green	o	n.s.	n.a.	n.a.	n.a.
		n.s.	n.a.	n.a.	n.a.
	+	n.s.	n.a.	n.a.	n.a.
Red	o	***	n.s.	***	***
		***	n.s.	***	***
	+	***	n.s.	***	***

n.a. post-hoc test not applied, n.s. $p > 0.05$, * $p \leq 0.05$, ** $p \leq 0.01$, *** $p \leq 0.001$

surprisingly high response. In general, many factors can play a role for the varying performance of certain wavelengths. The application of external pressure on the examined skin tissue, for example, might cause such variations. Previous cbPPG works show that the compression of superficial tissue leads to a significant change in the morphology and amplitude of the received signal [12, 15]. Moço et al. [15] argued that in this case, the cbPPG signal mostly arises from a deeper plexus due to the occlusion of superficial vessels. This theory could explain our outcome for the blue wavelengths. While contact sensors always apply pressure on the skin, setups for cbPPG usually do not. Therefore, superficial vessels still have an impact on the signal, especially for blue where the penetration depth is low and the absorption by hemoglobin high. However, Corral et al. [31] also used a contactless setup and did not report particular good qualities for the blue wavelength range. When applying the classic PPG theory to such results, the limited performance for blue can be attributed to its penetration depth where the light interacts less with pulsating vessels as longer wavelengths do [22, 23]. Since our results show better qualities for blue, the theory by Kamshilin et al. [12] might apply since capillaries in the papillary dermis are close enough to the surface to impact blue and green light with a similar strength [22, 23].

ROI location Based on the deviating results that we obtained for the lateral ROIs (see Table 4), we believe the cardiac signals in these regions to (partly) arise from sources other than those in the center ROI. The force of blood movement in the heart, the aorta and the great arteries causes a cyclic body movement [26] which is detectable on various body sites (BCG effects). Moço et al. [16] studied the presence of head-related BCG effects for facial areas and found that they are most prominent in case of inhomogeneous and non-orthogonal illumination. We expect to mostly receive such effects at the left and right ROI since the areas are not orthogonally aligned towards our light source. The dependency of the signal strength on the wavelength is, in comparison to the blood volume effects, minor for BCG effects. This characteristic explains the increase in the pulse strength of red up to the level of blue and green. Moço et al. [16] furthermore discovered that remnants of BCG effects were still present in the blue channel despite applying homogeneous illumination. Although this finding also could clarify the high response of the blue wavelengths for the center and full ROI, we are uncertain about why BCG effects would not have a similar influence on all three colors. Therefore, we favor the theory by Kamshilin et al. [12] as a possible explanation for the high response (see 'Color setting').

Although the left and right ROI provide qualitatively comparable results, differences in the filter setting between the regions are noteworthy. We believe this outcome also to be related to BCG effects. In contrast to BCG effects, blood volume effects require the light's interaction with the vascular structure. Therefore, we would not predict that polarization has the same impact on the BCG signal as it has on the blood volume signal. We assume the blood volume effect to be most present in the center and full ROI. Hence, regarding the outcome for the filter settings, the BCG effect must be dominant in the left ROI (filtration differences marginal) whereas, in the right ROI (filtration differences notable), both types of effects contribute more equally to the measured cbPPG signal. The disparity between the left and right ROI most likely originates from a systematic dislocation in our system setup. Our initial arrangement of the light source might have led minimally to a non-symmetrical illumination of the face. Consequently, the right forehead area was illuminated more orthogonally what caused a suppression of BCG effects. However, the results' tendency in both regions is still very similar when comparing it to the center ROI.

Filter setting Polarization filtration provides additional value to the investigation of establishing the signal's origin. The generally good performance of the '+' setting in the full and center ROI (for blue and green) supports the theory that cbPPG signals are mainly modulated by variations in the vasculature (i.e. beneath the surface) for these regions. Nevertheless, the cardiac

signal component in the '||' setting is still existent as corresponding p_{AC} values lie considerably above the noise level (see Fig. 4). The outcome would imply that cbPPG signals also arise from the skin surface. The following listing discusses this hypothesis by proving and disproving it:

- a) *BCG effect* If remnants of BCG effects are present in homogeneously illuminated areas, these effects will superimpose with blood volume effects. In this case, cardiac surface signals would be detectable and exclusively caused by BCG effects. However, Moço et al. [16] only found remnants in the blue range which would not explain our results for the green setting.
- b) *Depolarization* Although incident light gets depolarized in its direction when penetrating the skin, backscattered light can still contain a fraction of this direction when exiting the skin [6]. The fraction can be captured by the camera in the '||' setting and holds information from skin layers other than the surface. It would also be affected by hemoglobin's absorption, and we would predict a lower pulse strength for red.
- c) *Filter's extinction ratio* The extinction ratio of the polarization filters (see Table 1) shows that light can not be polarized perfectly. Therefore, non-polarized and polarized fractions from beneath the skin surface might enter the camera sensor in the '||' setting (similar to b)). However, due to the high extinction ratios, we assume this effect to be negligible.

In conclusion, we believe that the performance of the '||' setting is mostly explainable by point b).

Morphology analysis The contour analysis of the pulse waveform is an additional approach to draw conclusions about the cbPPG signal's origin [15]. In particular, the assessment of morphology changes between ROI locations, color and filter settings might provide a benefit in our study. However, the quantification of such changes across all subjects is complicated as certain shape characteristics vary strongly among individuals. Therefore, we exemplarily considered one participant where we believe the results to be a rough representation of peculiarities that we also found in other subjects. The mean beats of the chosen subject are visualized in Fig. 5, depicted for the various filter and color settings of the three ROI strips. For blue and green, the shape of the waveforms in the center ROI (second row) resemble the classic PPG waveform [3] which backs our claim that respective signals are modulated by blood volume changes. The filter setting has more impact on the beats' height rather than affecting the shape. For red, the contour is hard to characterize due to the low pulsation strength. In the left ROI, the waveforms are substantially different from those in the center ROI which mainly reflects in changes of phase and frequency (Fig. 5, first row). The outcome indicates BCG effects to be present, although the waveform of BCG signals is difficult to classify as it highly depends on the ROI location and the orientation of the light source [16, 17]. The slight shape variation between the filter and color settings further supports this theory as we similarly concluded earlier for p_{AC} . Based on the results for the pulse strength in the right ROI (see Fig. 4(d)), we stated that BCG and blood volume effects contribute more equally there. The waveforms of this subject (Fig. 5, third row) are in accordance with this assumption since they appear to be a mixture of the waveforms from the center and left ROIs. For red, the BCG effect seems to be dominant which not only reflects in the shape but also in the pulse strength (see center ROI for comparison). For blue and green, polarization filtration still causes an attenuation and augmentation of the waveforms.

5. Conclusion

We could show that in case of orthogonal illumination of the forehead, perpendicular polarization provides a significant benefit for the blue and green wavelengths in cbPPG. Furthermore, results

support the theory that signals most likely arise from blood volume changes. In case of non-orthogonal illumination, polarization has a smaller impact on the quality of cbPPG signals. This outcome can be associated with occurring BCG effects which are most prominent in the lateral regions. The effects also cause the signal's pulse strength to increase for the red wavelengths. CbPPG's response to polarization combined with its performance in various wavelengths is potentially a useful marker to distinguish between BCG affected signals and blood volume signals. For certain applications, BCG effects are not desirable (e.g. estimation of oxygen saturation) and have to be correctly identified. We want to note that some conclusions of our analysis can only be drawn for facial areas in case of being in an upright position. Therefore, prospective studies should consider different postures and investigate other anatomical regions.

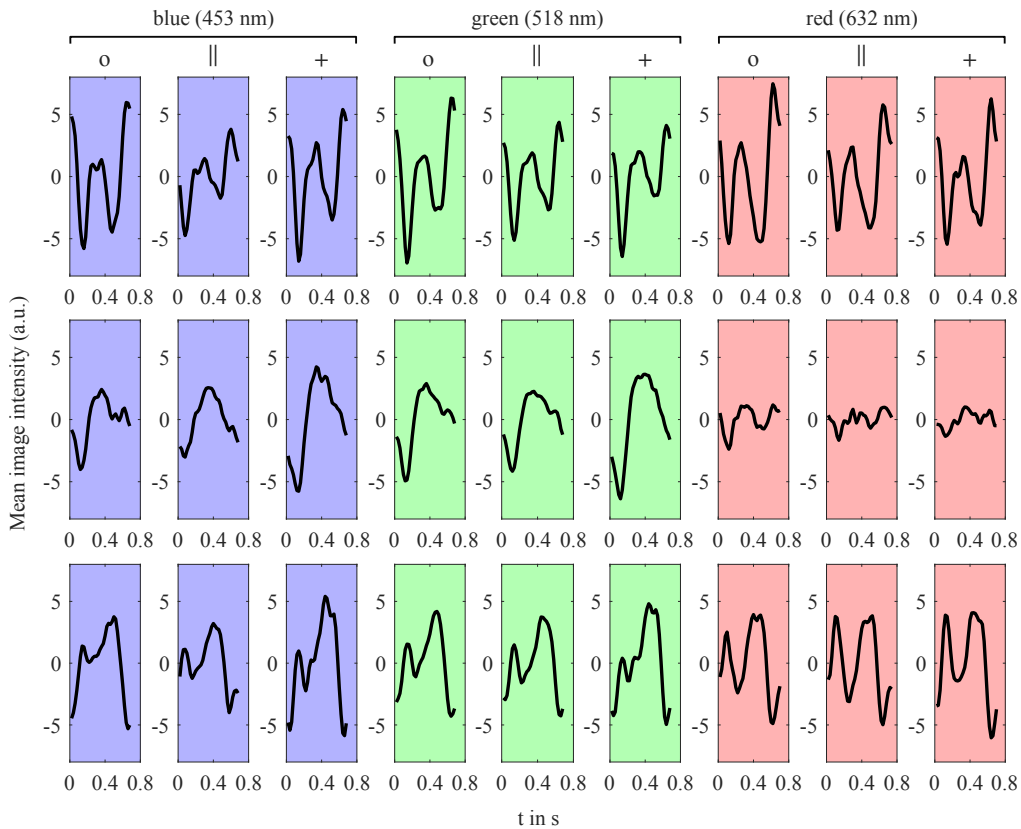


Fig. 5. Calculated mean beats of one subject for different ROIs, filter and color settings. The first row shows the results of the left ROI, the second row for the center ROI and the third row for the right ROI. The symbol 'o' represents the setting without polarization filters, '||' the parallel setting and '+' the perpendicular setting. The chosen color setting is represented by boxes' coloration and specified with their peak wavelengths (blue: 453 nm, green: 518 nm, red: 632 nm).

Funding

This work was funded by the "Staatsministerium für Wissenschaft und Kunst" (SMWK) of Saxony (project *CardioVisio*, ref. 4-7531.60/29/12) and the "Bundesministerium für Bildung und Forschung" (BMBF) (project *fast care - Kamerabasiertes Monitoring*, ref. 03ZZ0519C).